



## Article

# Structural and Mechanical Properties of NbN Alloyed with Hf, In, and Zr for Orthopedic Applications: A First-Principles Study

Adel Bandar Alruqi <sup>1,\*</sup>  and Nicholas O. Ongwen <sup>2</sup> <sup>1</sup> Department of Physics, Faculty of Science, King Abdulaziz University, Jeddah 21589, Saudi Arabia<sup>2</sup> Department of Physics, Masinde Muliro University of Science and Technology, Kakamega 50100, Kenya; info@mmust.ac.ke

\* Correspondence: aalruqi@kau.edu.sa

**Abstract:** The search for biocompatible, non-toxic, and wear-resistant materials for orthopedic implant applications is on the rise. Different materials have been investigated for this purpose, some of which have proved successful. However, one challenge that has proven difficult to overcome is the balance between ductility and hardness of these materials. This study employed ab initio calculations to investigate the structural and mechanical properties of niobium nitride (NbN) alloyed with hafnium, indium, and zirconium, with the aim of improving its hardness. The calculations made use of density function theory within the quantum espresso package's generalized gradient approximation, with Perdew–Burke–Ernzerhof ultrasoft pseudopotentials in all the calculations. It was found that addition of the three metals led to an improvement in both the shear and Young's moduli of the alloys compared to those of the NbN. However, both the bulk moduli and the Poisson's ratios reduced with the introduction of the metals. The Young's moduli of all the samples were found to be higher than that of bone. The Vickers hardness of the alloys were found to be significantly higher than that of NbN, with that of indium being the highest. The alloys are therefore good for wear-resistant artificial bone implants in ceramic acetabulum, and also in prosthetic heads.

**Keywords:** niobium nitride alloys; orthopedic application; mechanical properties of materials for orthopedic application; Vickers hardness; Hf-Nb-N alloys; In-Nb-N alloys; Zr-Nb-N alloys



**Citation:** Alruqi, A.B.; Ongwen, N.O. Structural and Mechanical Properties of NbN Alloyed with Hf, In, and Zr for Orthopedic Applications: A First-Principles Study. *Inorganics* **2024**, *12*, 43. <https://doi.org/10.3390/inorganics12020043>

Academic Editor: Xiangrong Chen

Received: 15 December 2023

Revised: 20 January 2024

Accepted: 23 January 2024

Published: 27 January 2024



**Copyright:** © 2024 by the authors. Licensee MDPI, Basel, Switzerland. This article is an open access article distributed under the terms and conditions of the Creative Commons Attribution (CC BY) license (<https://creativecommons.org/licenses/by/4.0/>).

## 1. Introduction

Advancements in medical technology have sparked the urge to better the lives of human beings. Orthopedic surgery is one of these developments, in which fractured or damaged bones can be replaced with artificial structures, which are mostly made from metallic biomaterials such as stainless surgical steel (because they are durable, non-toxic, ductile, and biocompatible), titanium alloys (since they bind well with adjacent bone, are corrosion-resistant, have elasticity that is comparable to that of bone, and are non-toxic), and cobalt–chromium–molybdenum (as they are biocompatible, have good wear, and are corrosion-resistant); ceramics such as aluminum oxide and zirconium oxide (since they are stiffer, have higher fracture toughness, are resistant to scratch and corrosion, as well as good biocompatibility); and polymeric biomaterials such as polythene and polytetrafluoroethylene (since they are non-corrosive, non-reactive, and biocompatible) are also employed [1]. These structures/materials should be strong enough to carry the body in addition to being non-toxic [2]. Stainless surgical steel remains to be the most widely used material for this purpose [3].

However, each of the above-mentioned materials has its own drawbacks. For instance, stainless steel does not have adequate resistance to corrosion in a biological environment. Moreover, it is relatively heavier compared to other materials used in the orthopedic implants such as titanium. Stainless steel is also highly radiopaque, meaning it obstructs X-rays and other medical imaging techniques, in addition to having limited elasticity or

flexibility compared to the other materials like titanium or certain alloys. This lack of elasticity can impact the ability of the implant to absorb and distribute forces, potentially leading to stress concentration or increased risk of implant failure. Titanium and its alloys, on the other hand, have been found to be more expensive compared to the other materials that are being utilized in orthopedic implants, such as stainless steel or the alloys of cobalt-chromium. They have a tendency to work-harden and cause rapid tool wear during the machining process, requiring specialized tools and techniques. This can increase manufacturing costs and time. The cobalt–chromium–molybdenum alloys are brittle, and are therefore susceptible to breaking during bending, making them poor candidates for bone fracture stabilization. Ceramics produce irritating squeaking during walking if they are used in joints, in addition to being inherently brittle, with low toughness. Polymers are highly ductile but have the disadvantage of having low strength as well as low elastic modulus. For instance, ultra-high molecular weight polythene has a Young’s modulus of only 0.7 GPa [4] compared to that of bone at 10–22 GPa [5].

Recently, niobium nitride (NbN) has been investigated as a prime candidate in the orthopedic surgery, where it has been alloyed with titanium (Ti-Nb-N), since it has been found to offer protection against wear allergies in load-bearing orthopedic devices such as artificial knees, hips, and shoulders. The Ti–Nb–N alloy has been found to possess some desirable properties such as corrosion resistance and full compatibility with the human body, besides being super elastic (being able to restore its original shape after large and repeated deformations) [6–8].

The desirable properties of materials for orthopedic applications include superior corrosion resistance, low degradability, high strength and low elastic modulus, good fatigue- and wear-resistance, high ductility, cytotoxicity, fracture toughness, high melting temperature, and tensile strength. NbN meets these properties, except two (poor wear resistance and low fracture toughness). While its high ductility (it has a very high Poisson’s ratio of 0.41) [9] is ideal for its ability to be molded into desired shapes for different regions of the body, it is prone to wear and fracture. Thus, it cannot perform well in ceramic acetabulum and prosthetic heads. In this study, we explored the mechanical properties of NbN alloyed with hafnium (Hf), indium (In), and zirconium (Zr), with the aim of improving its wear resistance. The three metals were chosen for doping NbN, since it has been reported that they have low toxicity [10–12]. This investigation’s specific goals were to ascertain (i) how hafnium, indium, and zirconium affected the NbN alloys’ structural properties, and (ii) how the above three elements affected the NbN alloys’ mechanical properties.

## 2. Results and Discussion

### 2.1. Structural Properties

For each of the four materials under consideration, Figure 1 shows the variation in total energy against normalized unit cell volumes. Among the four, In–Nb–N has the lowest total energy, making it the most stable. Zr–Nb–N was found to be the least stable. At the minima of the curves in Figure 1, the equilibrium lattice parameters were extracted, which are presented in Table 1. Table 1 clearly indicates that the lattice constants of NbN found in this investigation are in great agreement with the values found in the literature [9,13].

**Table 1.** The calculated lattice parameter, density, and  $c_{11}$ ,  $c_{12}$ , and  $c_{44}$  for all the samples.

Alloy	a (Å)	$\rho$ (kg/m <sup>3</sup> )	$c_{11}$ (GPa)	$c_{12}$ (GPa)	$c_{44}$ (GPa)
NbN	4.767	6452	$273.8 \pm 2.0$ 277.7 [9]	$192.3 \pm 1.3$ 189.8 [9]	$34.4 \pm 1.2$ 35.3 [9]
	4.76 [9]				
	4.76 [14]				
Hf-Nb-N	4.787	7440	$265.6 \pm 4.1$	$171.2 \pm 2.7$	$59.0 \pm 1.7$
In-Nb-N	4.821	6573	$213.4 \pm 1.4$	$150.0 \pm 2.5$	$72.4 \pm 1.1$
Zr-Nb-N	4.798	6402	$270.0 \pm 3.2$	$174.2 \pm 1.6$	$48.9 \pm 1.3$

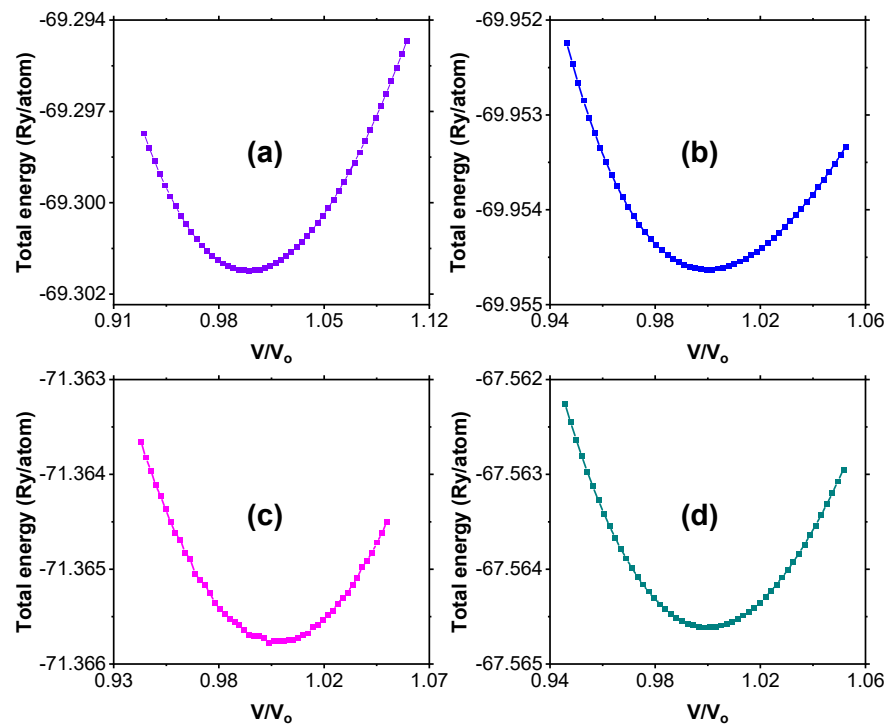


**Figure 1.** Total energy per atom as a function of the normalized unit cell volume (a) NbN, (b) Hf–Nb–N, (c) In–Nb–N, and (d) Zr–Nb–N.

The formation energy, which was calculated using Equation (1), was found to have a negative value ( $-0.7218$  Ry/atom), which indicates that NbN is structurally stable. Using the third order Birch–Murnaghan equation of state, the lattice constants of the alloys were derived by fitting the total energy–volume data. When the cell is fully relaxed, it contracted, since the estimated lattice parameter of NbN is 0.5217% less than the experimental reference value of  $4.792$  Å [14]. Since bone has a density of  $1900$  kg/m<sup>3</sup>, the density of NbN found in this work indicates that it is significantly a heavier material [15]. Strength, balance, and support for the body are among the advantages of having a higher bone density. Having better posture will make one appear more youthful and feel more energetic. Denser bones are ideal for the defense of the internal organs, and the assistance of the muscles, decreased likelihood of fragility fractures in old age, preventing bone loss, and even generating new bones. Thus, NbN and its alloys that have been explored here are good for bone replacement, since they are all much denser than bone.

Figure 2 shows the variation in the stresses and strains for the determination of elastic stiffness constants  $c_{ij}$  of the four materials in this study. It is clear from Figure 2 that  $c_{11}$  for NbN has the steepest slope and, therefore, it is expected to have the highest value of the elastic stiffness constant, while In–Nb–N is expected to have the lowest value.  $c_{12}$  is still dominated by NbN.  $c_{44}$ , on the other hand, is dominated by In–Nb–N. The elastic stiffness constants (and the uncertainties) were determined through linear fitting of the stress–strain data, as shown in the curves in Figure 2, and the data obtained are presented in Table 1.

Table 1 shows clearly that the elastic stiffness constants of NbN compare very well with those that are available in the literature [9,14]. It is worthwhile to note that after addition of the three metals to the NbN cell, the equilibrium lattice parameters increased. This is because addition of these metals led to expansion of the NbN, owing to their larger atomic radii (167 pm for hafnium, 166 pm for indium, and 160 pm for zirconium) compared to that of niobium at 146 pm. Addition of indium led to the highest expansion, as can be observed in Table 1.

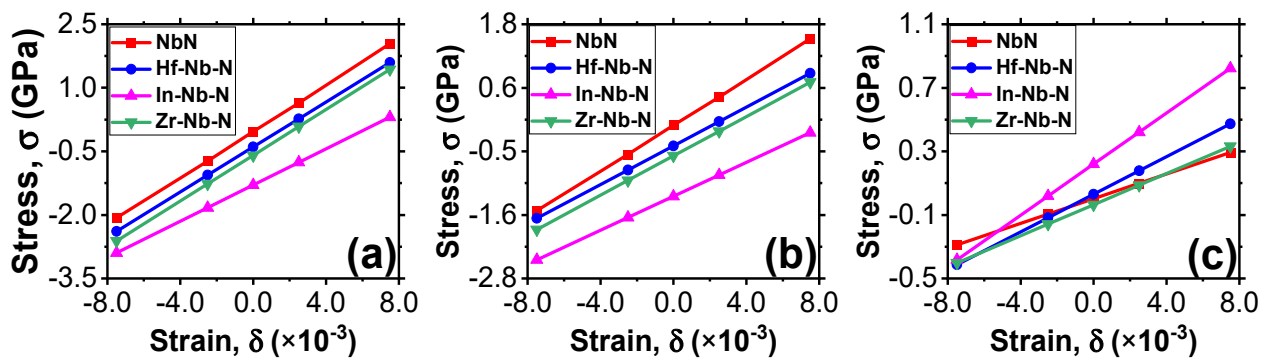


**Figure 2.** The curves of stress against strain for determination of stiffness constants  $c_{ij}$ : (a)  $c_{11}$ , (b)  $c_{12}$ , and (c)  $c_{44}$ .

Addition of zirconium lead to a decrease in the density of NbN, while addition of both hafnium and indium led to its increase. This was expected, since the density of zirconium at  $6510 \text{ kg/m}^3$  is less than that of niobium (at  $8580 \text{ kg/m}^3$ ). Substituting a denser atom with a less-dense atom was thus expected to lead to a decrease in the density of the doped cells. The densities of hafnium and indium are higher than that of niobium ( $13,310 \text{ kg/m}^3$  for hafnium and  $7310 \text{ kg/m}^3$  for indium), which are the reasons for the higher densities of Hf-Nb-N and In-Nb-N. Applying Equation (10)'s stability criterion, we arrived at the conclusion that all the samples examined in this investigation are mechanically stable.

All the samples had elastic stiffness constant  $c_{11}$  being greater than the other two, indicating that they are more resistant to changes in volume than changes in form. As a result, they had a high degree of incompressibility under uniaxial stress in the  $a$  direction. The highest value of  $c_{11}$  for NbN shows that it is the most incompressible (least compressible), while the lowest value for In-Nb-N shows that it is the least incompressible of all the alloys. Mechanical shear and the elastic stiffness constant,  $c_{12}$ , are connected. A high value of  $c_{12}$  indicates that a material is highly resistant to shear stress. Table 1 shows that NbN is the most resistant to shear stress, while In-Nb-N is the least. Bone tissues are usually subjected to tensile, compressive, and shear stresses during routine activities, whose magnitudes are often quite minor. However, when lengthy bones are torn, the stresses can reach significant levels. Long bone fractures can occur as a result of severe torsion. Torsional loads result in helical fracture surfaces, which result in a spiral fracture [5]. Thus, materials with higher values of  $c_{12}$  are better for the alleviation of fractures in bones. Pure NbN stands out in this regard since it has the highest value of  $c_{12}$ .

The elastic stiffness constant,  $c_{44}$ , indicates mechanical hardness. NbN exhibits the lowest value, which implies that it is the softest (least hard) of all the materials explored in this study. In-Nb-N possesses the highest value of  $c_{44}$ , which implies that it is the least soft (hardest) of all the materials presented here. Of all the three elastic stiffness constants,  $c_{44}$  was found to be the lowest. The much lower values of  $c_{44}$  indicates that the all the samples are relatively soft. Table 1 illustrates how well the estimated elastic stiffness constants for NbN acquired in this investigation match the data that are accessible in the literature, with very-low values of uncertainty.

## 2.2. Mechanical Properties

Table 2 displays the mechanical parameters of the samples, which were computed based on the elastic stiffness constants  $c_{ij}$ . Excellent agreement was discovered between the estimated mechanical parameters of NbN in this study and some from earlier research [9]. All the four materials examined in this study had quite-high bulk moduli, a measurement of a material's resistance to changing shape. This is an indication that the materials are resistant to fracture. NbN was found to have the highest bulk modulus and, therefore, is the most resistant to fracture, while In-Nb-N is the least resistant to fracture. Bone fracture is a common occurrence in bones, whose common cause is an impact or stress

with considerable force. However, those who have osteoporosis or bone cancer might develop bone fracture from very little impact [16]. As such, they are prone to fracture. The human femur has a bulk modulus of only 17 GPa [17]. Replacement of the fractured bones with biocompatible materials with higher resistance to fracture saves the risk of having subsequent fractures, including fractures on the artificial structures.

**Table 2.** The mechanical properties of the alloy samples. B stands for bulk modulus, G for shear modulus, E for Young’s modulus,  $n$  for Pugh’s modulus ratio, and  $H_V$  for Vickers hardness.

Alloy	B (GPa)	G (GPa)	E (GPa)	$\mu$	$n$	$H_V$ (GPa)
NbN	219.3	36.6	104.0	0.421	5.989	1.537
	219.1 [9]	38 [9]	109.0 [9]	0.41 [9]		1.649 [9]
Hf-Nb-N	202.7	54.0	171.2	0.377	3.576	3.445
In-Nb-N	171.1	52.0	141.5	0.362	3.292	3.896
Zr-Nb-N	206.1	48.5	134.9	0.391	4.250	2.773

The shear modulus, also referred to as the modulus of stiffness, is the proportion of shear stress to shear strain. Table 2 shows that the shear moduli of the doped NbN are superior to that of the pure NbN. Materials with high values of the shear modulus are characterized by extreme rigidity (also known as super hard materials) such as diamond. These materials have very-high thermal conductivity, compressive strength, and microhardness values [18]. Thus, all three of the alloys considered in this study are more rigid compared to NbN, which is ideal for bones such as the trabecular bone that is usually found at the end of long bones like the femur [19]. The typical values of the shear modulus of bone are 1.15 GPa for the subchondral, 4.59 GPa for the trabecular, and 5.44 GPa for the cortical [5]. These alloys are therefore ideal for replacement of damaged trabecular bone.

Young’s modulus is one of the most important material parameters for any technology application. The Young’s modulus is a metric for longitudinal tension resistance. In an ideal rigid body, the Young’s modulus would be infinite, meaning that much greater stress will be required to produce the same amount of strain. On the other hand, a very-soft substance (such a fluid) would deform naturally and, therefore, have no Young’s modulus [20]. Higher values of the Young’s modulus are ideal for the femur and the temporal bone of the skull. The Young’s moduli obtained in this study are relatively very high compared to that of the bone at 10–22 GPa [5]. They are therefore ideal as replacement for broken/fractured femurs or temporal bones of the skull. The Young’s moduli of the alloy samples were also found to be higher than that of the NbN, with that of Hf-Nb-N being the highest.

Since it typically falls between 0 and 0.5 for most materials, the Poisson’s ratio, which measures how much a material expands or contracts in directions perpendicular to the direction of force, is definitely high in this study at 0.362–0.421. This illustrates that even in the face of relatively minor strain, all the materials examined in this work exhibit significant elastic deformation. Such materials are referred to as ductile if they distort quickly while under slight tension. A material’s ductile/brittle properties can be determined using Poisson’s ratio. A brittle material has a value lower than 0.27, whereas a ductile material has a value higher than 0.27. The Pugh’s modulus ratios of the materials used in this investigation are also shown in Table 2. Brittleness is indicated by a Pugh’s ratio number of less than 1.75, and ductility is indicated by a value greater than 1.75 [21]. Since all of the materials used in this investigation complied with the two requirements for ductility, it was determined that they were all ductile.

The ability of bone to flex or stretch under tensile stress before breaking is gauged by its ductility. However, as tough and inflexible as it may be, bone does have some ductility. Bone can undergo plastic deformation, which means it can stretch or bend without breaking when subjected to slow and mild stresses. The bone will eventually fracture if the applied force is greater than its maximum tensile strength. The composition, age, and precise placement of the bone in the body are all factors that affect how ductile it is. Bone often has



lower ductility than substances like rubber or some metals. However, due to its hierarchical structure, bone exhibits a significant amount of toughness and may withstand fracture to some extent in comparison to other brittle materials. In contrast to other mechanical properties such as strength or stiffness, the ductility of bone is not commonly studied. When investigating bone biomechanics, researchers are primarily concerned with elements like bone density, elasticity, and fracture toughness. However, a Poisson's ratio of 0.62 has been reported for bone [22]. All the three metals investigated in this study were found to lower the ductility of NbN. However, all the values of ductility are well above the boundary of 0.27. Indium reduced it the most, while zirconium caused the least reduction.

Hardness is the ability of a material to withstand external mechanical forces that could potentially scratch, abrade, indent, or otherwise permanently modify its surface [23]. For bone, the low compressibility and good wear resistance of hard materials like diamond are highly desired. Hardness in bones is ideal because it provides protection of the organs such as the brain and the spinal cord, durability and resistance to wear, structural support and protection of vital body organs, and load-bearing function when the body is subjected to various mechanical activities such as walking and running [24]. However, while hardness is essential for the mechanical properties of bone, it must be balanced with other properties such as toughness and ductility.

The cubic NbN in the zinc blende structure that was studied in this work is characterized by very-low Vickers hardness, as can be observed in Table 2. It is therefore not suitable for artificial bone implant, since low Vickers hardness implies that it has low wear resistance. Addition of the three metals to NbN was found to significantly improve the Vickers hardness values of NbN. Indium was found to produce the largest increase in the Vickers hardness, while Zirconium was found to have the least increase. The Vickers hardness of Zr–Nb–N obtained in this study is much higher than that of bone at 33.3–43.8 Hv [25], corresponding to 0.3266–0.4295 GPa. It can thus form a good replacement for defective cortical bones such as the femur and tibia, which are dense and compact, since they are the major weight-bearing bones in the human body. This will enable them to effectively bear weight, provide stability, protect vital structures, and resist fatigue and fracture. These properties are essential for supporting locomotion and maintaining the overall strength and functionality of the lower limbs.

### 3. Materials and Methods

#### 3.1. Crystal Structures for Input

Starting with a NbN simple cell (Figure 3),  $2 \times 2 \times 2$  supercells were built in order to make the computation in this study possible. The NbN cell was a simple cube of the zinc blende phase, with an  $Fm-3m$  space group (number 225), containing 8 atoms (4 atoms of niobium and 4 atoms of nitrogen). The lattice parameter of the unit cell was 4.792 Å [14]. The supercells contained 64 atoms (32 of niobium and 32 of nitrogen), and they were then substitutionally doped by replacing 6 of the niobium atoms with 6 atoms of hafnium, indium, and zirconium separately in three different supercells. The modelling was performed using the SOD (site-occupation disorder) algorithm [26]. The supercells were given sample numbers of Hf–Nb–N, In–Nb–N, and Zr–Nb–N. Figure 4 shows the doped supercells. The doping was performed with the help of Burai 1.3.2 (a Quantum Espresso graphical user interface).

Doping of the supercells was conducted in such a way that the supercells remained cubic. This was achieved by replacing the Nb atoms (with hafnium, indium, and zirconium) along the symmetry lines of the crystal. The bonds between the dopants and niobium or nitrogen were also not broken in the process of doping. This is because the dopants are large atoms, which are almost the same size as that of niobium. Thus, the dopants were able to fit into the vacancy left by niobium.

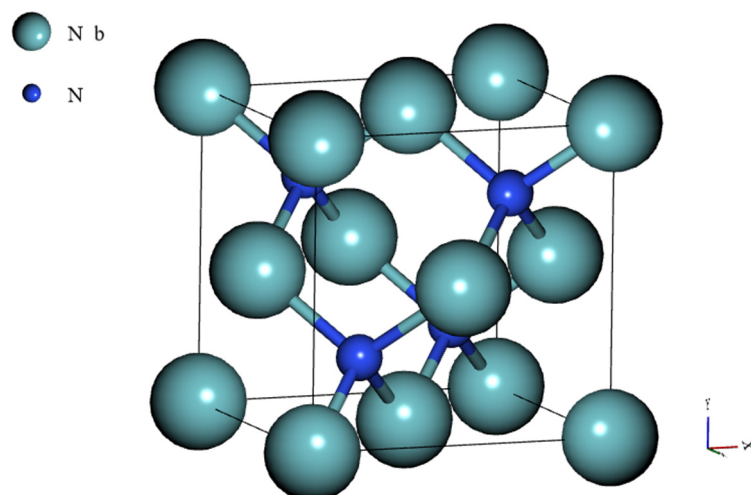


**Figure 3.** The crystal structure of the cubic NbN crystal structure viewed by Burai.

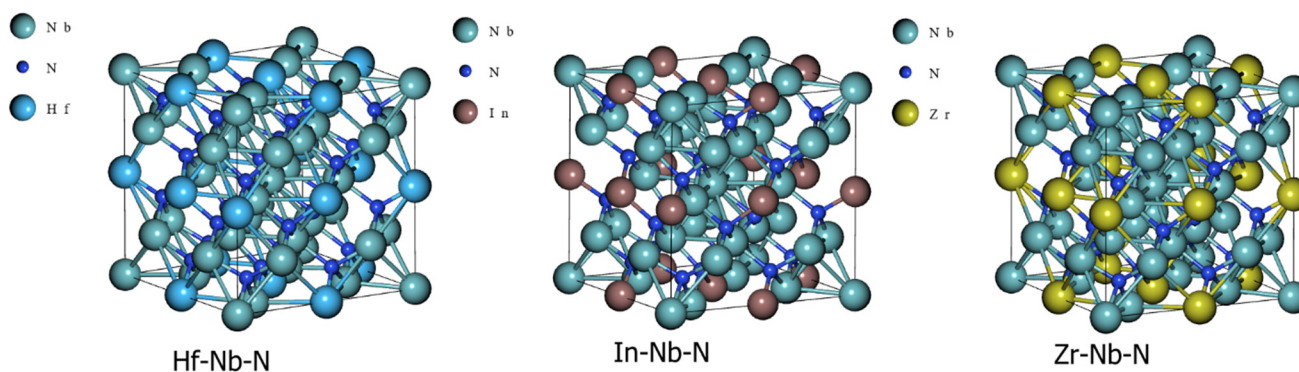


**Figure 4.** The crystal structures of the three supercells viewed by Burai.

Because there were many atoms (64 in total) in each supercell, a moderate kinetic energy cut-off of 50 Ry and an unshifted Monk-host Pack mesh [27] of  $5 \times 5 \times 5$  were used in all of the supercells. We applied density functional theory under the generalized gradient approximation for all the calculations. The Perdew–Burke–Ernzerhof (PBE) functionals [28] were employed in this study. Scalar relativistic PBE ultrasoft pseudopotentials were utilized.

The doped supercells were then subjected to structural optimization, where a variable cell relaxation was applied to them in order to relax the lattice points and the lattice parameters. This was made possible using the Broyden–Fletcher–Goldfarb–Shanno algorithm, with a pressure of 0.00 GPa and a pressure convergence threshold of 0.05 GPa. The cutoff values for charge density and kinetic energy were established at 50 Ry and 400 Ry, respectively. The charge density cut-off was determined through multiplying the kinetic energy cut-off by 8, since the pseudopotentials employed here were ultrasoft. The forces operating on the atoms at the conclusion of the optimization were within  $\times 10^{-3}$  Ry/au.

We computed the formation energy ( $E_F$ ) of the NbN phase so as to assess its structural stability. The procedure involved calculating the total energies of the optimized unit cells of NbN, nitrogen, and niobium, then inserting the total energies into Equation (1):

$$E_F = \sum A - \sum B - \sum C, \quad (1)$$

in which  $A$ ,  $B$ , and  $C$  represent NbN, Nb, and N, respectively. The nitrogen cell was a simple cube of nitrogen atom.

### 3.2. Calculation of Mechanical Properties

Solid materials resist external forces that have a tendency to distort them [29]. A material's elastic properties determine how it reacts to external loads and can be used in a variety of ways. Hooke's law governs the elastic properties of materials. It asserts that the stresses  $\sigma_i$  in a material are proportional to the corresponding applied strains  $\delta_j$  within the linear domain of the crystal. One way to express the law is as follows:

$$\sigma_i = \sum_{j=1}^6 c_{ij} \delta_j, \quad (2)$$

in which  $c_{ij}$  are the elastic stiffness constants. By applying stress to the lattice vector  $R$  using the formula  $R' = RD$ , where  $D$  is the symmetric distortion matrix that contains the strain components and  $R'$  is a matrix holding the elements of the deformed lattice vectors, one can obtain the combined linear elastic constants.

Computation of elastic constants (and consequently, the mechanical properties) in this study employed the stress–strain approach of Ongwen, Ogam, and Otunga [30]. For each supercell, the strains given to the equilibrium crystals ranged from  $-0.0075$  to  $+0.0075$  in increments of  $0.0025$ . The tensions were then determined. The elastic stiffness constants ( $c_{ij}$ ) could be obtained by linearly fitting the stress–strain data.

Only three distinct elastic stiffness constants ( $c_{11}$ ,  $c_{12}$ , and  $c_{44}$ ) were required in order to ascertain the elastic constants and, in turn, the mechanical properties of the materials for the cubic crystals. According to Voigt [31] and Reus [32], there is the following connection between the elastic constants and elastic stiffness constants:

$$B_V = B_R = \frac{1}{3}(c_{11} + 2c_{12}), \quad (3)$$

$$G_V = \frac{1}{5}(c_{11} - c_{12} + 3c_{44}), \quad G_R = \frac{5(c_{11} - c_{12})c_{44}}{4c_{44} + 3(c_{11} - c_{12})}, \quad (4)$$

where  $B_V$  and  $B_R$  stand for the Voigt and Reuss shear moduli, and  $G_V$  and  $G_R$  for the Voigt and Reuss bulk moduli, respectively. Muslov, Lotkov, and Arutyunov [33] found the following connection between the elastic stiffness constants and the elastic compliance constants ( $S_{ij}$ ) for cubic crystals:

$$s_{11} = \frac{c_{11} + c_{12}}{(c_{11} - c_{12})(c_{11} + 2c_{12})} \quad (5)$$

$$s_{12} = \frac{-c_{12}}{(c_{11} - c_{12})(c_{11} + 2c_{12})} \quad (6)$$

$$s_{44} = \frac{1}{c_{44}} \quad (7)$$

The Hill's approximation [34] is the result of averaging the two approximations:

$$B = \frac{B_V + B_R}{2}, \quad G = \frac{G_V + G_R}{2} \quad (8)$$

The resultant Young's modulus ( $E$ ) and Poisson's ratio ( $\nu$ ) are obtained using the relationships given by Chen et al. [35], using the computed bulk and shear moduli:

$$E = \frac{9BG}{3B + G}, \quad \nu = \frac{3B - 2G}{2(3B + G)} \quad (9)$$

The mechanical stability of cubic crystals is governed by the following stability criteria [36,37]:

$$c_{11} + 2c_{12} > 0, \quad c_{44} > 0, \quad c_{11} > |c_{12}| \quad (10)$$



The Vickers hardness (for determining the wear resistance) in this study was determined using the Tian model [38]:

$$H_v = 0.92k^{1.137}G^{0.708} \quad (11)$$

where  $k = G/B'$  the reciprocal of the Pugh's modulus ratio.

#### 4. Conclusion

This study successfully showed that through alloying of NbN, it is possible to come up with artificial orthopedic implants that are ductile, in addition to having higher wear resistance as a result of their improved Vickers hardness. This study demonstrated that indium is the best in producing a NbN alloy among the three metals, with a Vickers hardness that is much higher than that of bone. The addition of the three metals led to an increase in the Young's modulus, shear modulus, and Vickers hardness, while the bulk modulus and Poisson ratio reduced. The higher densities Hf–Nb–N and In–Nb–N are good for stronger materials as a replacement for fractured bones. However, since there are many factors that determine the suitability of a structure for orthopedic implant application, other factors such as toxicity and irritancy of the modelled materials need to be investigated since they were not considered in this study.

**Author Contributions:** Conceptualization, A.B.A.; methodology, N.O.O.; software, A.B.A. and N.O.O.; validation, A.B.A.; formal analysis, A.B.A. and N.O.O.; investigation, A.B.A.; resources, A.B.A. and N.O.O.; data curation, A.B.A.; writing—original draft preparation, A.B.A. and N.O.O.; writing—review and editing, A.B.A.; visualization, A.B.A. All authors have read and agreed to the published version of the manuscript.

**Funding:** This research work was funded by Institutional Fund Projects under grant no. (IFPIP:1549-130-1443). The authors gratefully acknowledge technical and financial support provided by the Ministry of Education and King Abdulaziz University, DSR, Jeddah, Saudi Arabia.

**Data Availability Statement:** Data are contained within the article.

**Conflicts of Interest:** The authors declare no conflicts of interest.

#### References

1. Szczesny, G.; Kopec, M.; Politis, D.J.; Kowalewski, A.; Szolc, T. A review of biomaterials for orthopedic surgery and traumatology: From past to present. *Materials* **2022**, *15*, 3622. [CrossRef]
2. Badhe, R.V.; Akinfosile, A.; Bijukumar, D.; Barba, M.; Mathew, M.T. Systemic toxicity eliciting metal ion levels from metallic implants and orthopedic devices—A mini review. *Toxicol. Lett.* **2021**, *310*, 213–224. [CrossRef] [PubMed]
3. Geanta, V.; Voiculescu, I.; Ștefănoiu, R.; Rusu, E.R. Stainless steels with biocompatible properties for medical devices. *Key Eng. Mater.* **2013**, *583*, 9–15. [CrossRef]
4. Buechel, F.F.; Pappas, M.J. Properties of materials used in orthopedic implant systems. In *Principles of Human Joint Replacement*; Springer: Cham, Switzerland, 2015. [CrossRef]
5. Ma, C.; Du, T.; Niu, X.; Fan, Y. Biomechanics and mechanobiology of the bone matrix. *Bone Res.* **2022**, *10*, 59. [CrossRef] [PubMed]
6. Thienpont, E. Titanium niobium nitride knee implants are not inferior to chrome cobalt components for primary total knee arthroplasty. *Arch. Orthop. Trauma. Surg.* **2015**, *135*, 1749–1754. [CrossRef] [PubMed]
7. Yamini, S.A. Influence of microalloying elements (Ti, Nb) and nitrogen concentrations on precipitation of pipeline steels—A thermodynamic approach. *Eng. Rep.* **2020**, *3*, e12337. [CrossRef]
8. Buscaglia, V. Nitridation of Ti/Nb alloys and solid-state properties of  $\delta$ -(Ti,Nb)N. *J. Alloys Compd.* **1997**, *262–263*, 521–528.
9. Muchiri, P.W.; Mwalukuku, V.M.; Korir, K.K.; Amolo, G.O.; Makau, N.W. Hardness characterization parameters of niobium carbide and niobium nitride: A first principles study. *Mater. Chem. Phys.* **2019**, *229*, 489–494. [CrossRef]
10. Field, J.A.; Luna-Velasco, A.; Boitano, S.A.; Shadman, F.; Ratner, B.D. Cytotoxicity and physicochemical properties of hafnium oxide nanoparticles. *Chemosphere* **2011**, *84*, 1401–1407. [CrossRef]
11. Lim, C.H.; Han, J.-H.; Cho, H.-W.; Kang, M. Studies on the toxicity and distribution of indium compounds according to particle size in sprague-dawley rats. *Technol. Res.* **2015**, *30*, 55–63. [CrossRef]
12. Yang, Y.; Bao, H.; Chai, Q.; Wang, Z.; Sun, Z.; Fu, C.; Liu, Z.; Mung, X.; Liu, T. Toxicity, biodistribution and oxidative damage caused by zirconia nanoparticles after intravenous injection. *Int. J. Nanomed.* **2023**, *14*, 5175–5186. [CrossRef]

13. Korir, K.K.; Amolo, G.O.; Makau, N.W.; Joubert, D.P. First-principles calculations of the bulk properties of 4d transition metal carbides and nitrides in the rock salt, zincblende and wurtzite structures. *Diam. Relat. Mater.* **2011**, *20*, 157–164. [[CrossRef](#)]
14. Becker, K.; Ebert, F. Die Kristallstrukturen einiger binärer Carbide und Nitride. *Z. Für Phys.* **1925**, *31*, 268–272. [[CrossRef](#)]
15. Cameron, J.R.; Skofronick, J.G.; Grant, R.M. *Physics of the Body*; Medical Physics Publishing: Madison, WI, USA, 1999.
16. Oryan, A.; Monazzah, S.; Bigham-Sadegh, A. Bone injury and fracture healing biology. *Biomed. Environ. Sci.* **2015**, *28*, 57–71. [[CrossRef](#)] [[PubMed](#)]
17. Gaith, M.; Al-Hayek, I. Elastic comparison between human and bovine femoral bone. *Res. J. Appl. Sci. Eng. Technol.* **2012**, *4*, 5183–5187.
18. Lu, C.; Chen, C. Structure-strength relations of distinct MON phases from first-principles calculations. *Phys. Rev. Mater.* **2020**, *4*, 1–13. [[CrossRef](#)]
19. Hart, H.H.; Nimphius, S.; Rantalainen, T.; Ireland, A.; Siafarikas, A.; Newton, R.U. Mechanical basis of bone strength: Influence of bone material, bone structure and muscle action. *J. Musculoskelet. Neuronal. Interact.* **2017**, *17*, 114–139. [[PubMed](#)]
20. Wang, J.; Zhou, B.; Parkinson, I.; Thomas, C.D.L.; Clement, J.G.; Fazzalari, N.; Guo, X.E. Trabecular plate Loss and deteriorating elastic modulus of femoral trabecular bone in intertrochanteric hip fractures. *Bone Res.* **2013**, *1*, 346–354. [[CrossRef](#)] [[PubMed](#)]
21. Pugh, S.F. XCII. Relations between the elastic moduli and the plastic properties of polycrystalline pure metals. *Lond. Edinb. Dublin Philos. Mag. J. Sci.* **1954**, *45*, 823–843. [[CrossRef](#)]
22. Morgan, E.F.; Unnikrisnan, G.U.; Hussein, A.I. Bone mechanical properties in healthy and diseased states. *Annu. Rev. Biomed. Eng.* **2018**, *20*, 119–143. [[CrossRef](#)]
23. Oganov, A.R.; Lyakhov, A.O. Towards the theory of hardness of materials. *J. Superhard Mater.* **2010**, *32*, 143–147. [[CrossRef](#)]
24. Ibrahim, A.; Magliulo, N.; Groben, J.; Padilla, A.D.; Akbik, F.; Hamid, Z.A. Hardness, an important indicator of bone quality, and the role of collagen in bone hardness. *J. Funct.* **2020**, *11*, 85. [[CrossRef](#)]
25. Wu, W.; Zhu, Y.; Chen, W.; Li, S.; Yin, B.; Wang, J.; Zhang, X.; Liu, G.; Hu, Z.; Zhang, Y. Bone hardness of different anatomical regions of human radius and its impact on the pullout strength of screws. *Orthop. Surg.* **2019**, *11*, 270–276. [[CrossRef](#)] [[PubMed](#)]
26. Grau-Crespo, R.; Hamad, S.; Catlow, C.R.A.; de Leeuw, N.H. Symmetry-adapted configurational modelling of fractional site occupancy in solids. *J. Phys. Condens. Matter.* **2007**, *19*, 256201. [[CrossRef](#)]
27. Monkhorst, H.J.; Pack, J.D. Special points for Brillouin zone integration. *Phys. Rev. B* **1976**, *13*, 5188. [[CrossRef](#)]
28. Sun, J.; Remsing, R.C.; Zhang, Y.; Sun, Z.; Ruzsinszky, A.; Peng, H.; Yang, Z.; Paul, A.; Waghmare, U.; Wu, X.; et al. Accurate first-principles structures and energies of diversely bonded systems from an efficient density functional. *Nat. Chem.* **2016**, *8*, 831–836. [[CrossRef](#)]
29. Bouchenafa, M.; Benmakhlouf, A.; Sidoumou, M.; Bouchemadou, A.; Maabed, S.; Halit, M.; Bentabet, A.; Bin-Omran, S.; Khenata, R.; Al-Douri, Y. Theoretical investigation of the structural, elastic, electronic and optical properties of the ternary tetragonal tellurides  $\text{KBTe}_2$  (B = Al, In). *Mater. Sci. Semicond. Process.* **2020**, *114*, 105085. [[CrossRef](#)]
30. Ongwen, N.O.; Ogam, E.; Otunga, H. Ab initio study of elastic properties of orthorhombic cadmium stannate as a substrate for the manufacture of MEMS devices. *Mater. Today Commun.* **2021**, *26*, 101822. [[CrossRef](#)]
31. Voigt, W. *Lehrbuch der Kristallphysik*; B.G. Teubner: Leipzig/Berlin, Germany, 1928.
32. Reuss, A. Calculation of the flow limits of mixed crystals on the basis of the plasticity of monocrystals. *J. Appl. Math. Mech.* **1929**, *9*, 49–58.
33. Muslov, S.A.; Lotkov, A.I.; Arutyunov, S.D. Extrema of elastic properties of cubic crystals. *Russ. Phys. J.* **2019**, *62*, 1417–1427. [[CrossRef](#)]
34. Hill, R.W. The elastic behaviour of a crystalline aggregate. *Proc. Phys. Soc. A* **2002**, *65*, 349. [[CrossRef](#)]
35. Chen, W.-H.; Yu, C.-F.; Chiang, K.-N.; Cheng, H.-C. First-principles density functional calculations of physical properties of orthorhombic  $\text{Au}_2\text{Al}$  crystal. *Intermetallics* **2015**, *62*, 60–68. [[CrossRef](#)]
36. Grimvall, G.; Magyari-Köpe, B.; Ozoliņš, V.; Persson, K.A. Lattice instabilities in metallic elements. *Rev. Mod. Phys.* **2012**, *84*, 945–986. [[CrossRef](#)]
37. Wang, J.; Li, J.; Yip, S.; Phillpot, S.; Wolf, D. Mechanical instabilities of homogeneous crystals. *Phys. Rev. B* **1995**, *52*, 12627. [[CrossRef](#)]
38. Avery, P.; Wang, X.; Oses, C.; Gossett, E.; Proserpio, D.M.; Toher, C.; Curtarolo, S. Predicting superhard materials via a machine learning informed evolutionary structure search. *Comput. Mater.* **2019**, *5*, 89. [[CrossRef](#)]

**Disclaimer/Publisher’s Note:** The statements, opinions and data contained in all publications are solely those of the individual author(s) and contributor(s) and not of MDPI and/or the editor(s). MDPI and/or the editor(s) disclaim responsibility for any injury to people or property resulting from any ideas, methods, instructions or products referred to in the content.